

# A Bioluminescent Orthotopic Mouse Model of Human Osteosarcoma that Allows Sensitive and Rapid Evaluation of New Therapeutic Agents *In Vivo*

KENINE E. COMSTOCK, CHRISTOPHER L. HALL, STEPHANIE DAIGNAULT,  
SARAH A. MANDLEBAUM, CHUNYAN YU and EVAN T. KELLER

*Department of Urology/Surgery, University of Michigan, Ann Arbor, MI 48118, U.S.A.*

**Abstract.** *Osteosarcoma (OSA) is the most common primary malignant bone tumor in children, 30% of whom develop lung metastases despite aggressive treatment. Our objective was to develop a mouse model of OSA for preclinical studies that (i) incorporates the natural history of OSA including tumor growth in bone and development of lung metastasis and (ii) is amenable to non-invasive detection methods. A human OSA cell line that expresses high levels of luciferase was created. Following subcutaneous injection, nine out of ten mice showed tumor growth. Eight out of ten mice showed tumor growth following orthotopic injection into the proximal tibia. Thirty percent of mice showed pulmonary metastasis by bioluminescent imaging eight to 10 weeks following orthotopic injection. Animals receiving cisplatin treatment showed reduced tumor volume compared to animals treated with vehicle alone. This model allows real-time detection of tumors and can be used to study mechanisms of OSA metastasis and test new therapeutic agents.*

Osteosarcoma (OSA) is the second leading cause of cancer-related death in children, affecting primarily adolescents. There are an estimated 1,500 cases per year occurring in the United States, accounting for about 3.5% of all cancer cases in those under 20 years of age (1, 2). OSA also occurs in older adults, although at a lower frequency. The age distribution of OSA shows the highest incidence at 10-19 years of age while a second but lower peak in incidence occurs in the 7th decade of life (2). The distal femur, proximal tibia and proximal humerus are the most common primary sites of occurrence in humans.

*Correspondence to:* Evan T. Keller, University of Michigan, 5308 Cancer Center, 1500 E Medical Center Dr., Ann Arbor MI 48109, U.S.A. Tel: +1 734 6150280, e-mail: etkeller@umich.edu

*Key Words:* Osteosarcoma, bone cancer, animal models, non-invasive imaging, pulmonary metastasis.

Treatment of OSA remains difficult. Five-year survival has increased from approximately 15% in the 1950s with surgical management to approximately 60% in the 1980s from inclusion of adjuvant chemotherapy, notably doxorubicin, methotrexate and cisplatin, in the treatment but has not changed recently due to the slow development of improved chemotherapies (3-5). One-third of patients diagnosed with OSA will develop pulmonary metastases that lead to death. Five-year survival for those presenting with pulmonary metastasis at diagnosis is less than 20% (6). The low survival rate of patients with OSA metastasis indicates that there is much room for improvement in the treatment of advanced and relapsed OSA. Most likely, this will involve the development of new drug therapies and the improvement of diagnostic and prognostic tools by making use of preclinical models of OSA.

Animal models of OSA are critical for preclinical evaluation of therapeutic agents as relatively small numbers of children develop OSA and thus make clinical trials challenging to perform. However, few OSA models currently exist for studying the pathobiology of OSA tumor progression, metastasis and identifying anti-OSA agents. For a model to have the best chance at being predictive of clinical outcome, it should demonstrate the characteristics of the cancer in a human patient including histologic type and tendency to spontaneously metastasize. In addition, confirmation of the model's response to therapeutic drugs effective in treating OSA is an important step to validate the model for use in preclinical studies. It has been proposed that the use of panels of xenograft models that both mimic the characteristics of primary tumor and reflect the inherent variability in these types of cancer might be of more predictive value when testing new therapeutic agents (7). Accordingly, we explored the potential to add to and improve upon the currently available preclinical models of OSA.

## Materials and Methods

*Cell lines.* OS187, a human OSA cell line, was a gift from R. Gorlick (Albert Einstein College of Medicine, New York, NY, USA). OS187 was derived from a diagnostic, pre-treatment biopsy of the ilium of

a 17-year-old male who presented with multiple bone lesions and pulmonary metastases. The biopsied lesion was believed to be the primary site of disease, but the presence of multiple bone metastases, many of which were large in size, confounded identification of the primary OSA.

All cell lines (OS187 and OS187-luc) were maintained in Dulbecco's modified Eagle's medium (DMEM) supplemented with 10% fetal bovine serum, 100 mg/ml penicillin G sodium and 100 mg/ml streptomycin sulfate, 2.0 mM L-glutamine, and 10% insulin-transferrin-selenium-X (Invitrogen, Corp., Carlsbad, CA, USA) in a 5% CO<sub>2</sub> and 95% air atmosphere at 37°C.

*Establishment of stably transduced OSA cells expressing the LUC reporter gene.* Exponentially-growing OS187 cells were transduced with a retrovirus containing the luciferase gene driven by the LTR promoter (gift from J. Nor, University of Michigan) in the presence of 4 µg/ml polybrene (Sigma-Aldrich, St. Louis, MO, USA). Cells were allowed to recover for 24 hours, then medium containing 1 µg/ml G418 Sulfate (Invitrogen, San Diego CA, USA) was added. Cells were grown in selective media until a parallel culture of uninfected control cells were dead (10 days). At this point cells were cloned in 96-well plates by limiting dilution. Populations were expanded, then assayed *in vitro* for luciferase activity using the Dual-Luciferase Reporter Assay System (Promega Corp., Madison WI, USA). The clonal population showing the highest level of activity was used for all subsequent experiments.

*Subcutaneous and orthotopic intratibial injections.* Six weeks old female athymic nude (Nu/Nu) mice were purchased from Charles River Laboratories, Inc. (Wilmington, MA, USA). All animal experiments were approved by the University of Michigan IACUC. For both subcutaneous and intratibial injections, exponentially growing cells were harvested, counted and resuspended in serum-free media to a final density of 1×10<sup>7</sup> cells/ml. Anesthesia was induced using a 1.5% isoflurane-air mixture. For subcutaneous cells were injected into the right flank. For intratibial injection, the cortex of the tibial crest was penetrated using a 27-gauge needle, then using a second needle, 50 µl containing 5×10<sup>5</sup> cells were injected as previously described (8).

*Radiographic evaluation.* Radiographic images were obtained using a cabinet X-ray system (Faxitron, Wheeling, IL, USA) and X-OMAT film (Eastman Kodak, Rochester, NY, USA). Radiographic exposures were performed at 23 kVp for 7.5 seconds.

*Bioluminescence imaging (BLI).* Mice were injected intraperitoneally with 4 mg/kg luciferin (Xenogen, Alameda CA, USA) dissolved in phosphate buffered saline (PBS). Anesthesia was induced and maintained using a 1.5% isoflurane-air mixture. The mice were transferred to a light impermeable imaging chamber and readings were obtained 12 minutes following luciferin administration. Imaging was performed with all mice in a dorsal position. For subcutaneous tumors, images were obtained once weekly for 9 weeks following injection. For intra-tibial tumors, after an initial period of two weeks following injection of tumor cells, images were obtained once weekly for 5 weeks. Animals were euthanized when the tumor volume began to influence health status and mobility or at the end of the study period, which was nine weeks for subcutaneous tumors or seven weeks for intra-tibial tumors.

*Histopathology.* Tumors were excised at necropsy and preserved in 10% formalin (Sigma-Aldrich). Tissues were prepared by paraffin preparation, sectioning, and hematoxylin and eosin staining. Slides were analyzed microscopically using a Nikon Eclipse EC400 microscope.

*Measurement of subcutaneous tumor volume.* Subcutaneous tumors were measured weekly using calipers to monitor growth. The tumors were measured in length and width at the same location by the same technician each time. Tumor volume was calculated using the formula: (min)<sup>2</sup>(max)/2 (9).

*Drug treatment.* Twenty-two female nude mice were orthotopically injected with OS187-luc cells as described above. After 8 days, mice were injected with either 8.0 mg/kg cisplatin (II) diaminodichloride (Bedford Laboratories, Bedford, OH USA) with vehicle alone weekly into the peritoneal cavity (IP) for four weeks total. Tumor growth was monitored by BLI using the techniques described above.

*Statistical methods.* The association between BLI and caliper methods to measure tumor size was analyzed using Spearman's rank correlation, which is a non-parametric measure of correlation that does not assume a linear relationship between the BLI and caliper measurements. Spearman's rank correlations were calculated for the overall data, for each mouse over time, and for each time point over all mice.

For the drug treatment study, a generalized linear mixed model was used to model tumor growth with and without cisplatin treatment to account for the repeated measures over time among the mice. Parameters in the model include treatment, linear and quadratic terms for time and interactions between the time terms and treatment. Model estimates are reported. Contrasts were used to test for differences between the treatment groups each week. All statistical analysis was performed using SAS 9.1 (SAS Institute, Cary, NC, USA).

## Results

Bioluminescent imaging (BLI) is a technique that can be used to non-invasively measure characteristics of tumor growth and metastasis. In order to utilize BLI, we engineered OS187 to constitutively express luciferase at a level suitable for highly sensitive BLI. This was achieved by infecting exponentially-growing OS187 cells with a replication incompetent retrovirus containing the luciferase gene driven by the LTR promoter and a neo cassette. Cells were selected in G418, assayed *in vitro* for luciferase activity and subsequently referred to as OS187-luc.

We next assessed (i) the ability of OS187-luc to form tumors following subcutaneous injection and (ii) the correlation between volume measured using calipers *versus* tumor burden as determined using BLI. Ten athymic female nude mice were injected with exponentially growing cells in the lower right flank. Tumor growth was then monitored by both BLI and caliper measurement weekly. Nine out of ten mice showed subcutaneous tumor growth. Luminescence

increased in the tumor injection site over time (Figure 1A). BLI strongly correlated with caliper measurement (Figure 1B and 1C). The overall Spearman correlation was strongly positive  $R=0.84$ . Most mice (7/10) showed a strong positive correlation between the BLI and caliper measurement methods ( $R\geq 0.80$ ). Mouse #2 showed no tumor growth by either method and therefore had a correlation of 1. Mice #3 and #4 gave R values of 0.851 and 0.885, respectively. Both #3 and #4 showed no bioluminescence at two time points with positive tumor growth by caliper measurement. This may have been due to problems with circulation of the luciferin substrate following intraperitoneal injection or an operator error in the injection site. Mouse #5, which had correlation of 0.325, showed very rapid tumor growth by BLI and caliper measurement. The large size of the tumor may have resulted in attenuation of bioluminescent light emission with increased tissue depth and/or necrosis at the later time points.

We next wanted to compare the efficacy of BLI *versus* caliper measurement at both early and late tumor growth time points. Tumor measurements at 14 days gave a lower correlation between methods than tumor measurements at 21 days (Figure 2). We hypothesize that the lower correlation at 14 days occurred because increased high sensitivity of BLI allowed detection earlier than the caliper method did. In those nine mice that developed a tumor, the tumor was detected an average of 12.5 days earlier using BLI compared with caliper measurement. At 21 days, both methods were able to detect the tumor in mice that grew a tumor. The strength of the correlation decreased at later time points. At 53 days and later, the correlation was poor ( $R\leq 0.4$ ).

In order for an animal model of cancer to be useful for assessing the utility of new therapeutic agents, it should exhibit the growth and biological characteristics of the tumor in a human patient and emulate the clinical progression of the disease. Since one of the most common locations of primary tumor is the proximal tibia in humans, we assessed the ability of OS187-luc cells to form tumors when injected orthotopically into the tibia of ten nude mice. Tumor growth was monitored weekly starting at two weeks' post-injection by both BLI and radiography. The increased sensitivity of BLI permitted detection of occult tumor growth on average three weeks earlier than radiography. At two weeks, five out of the ten mice showed detectable bioluminescence. Seven out of ten mice showed tumor growth as detected by BLI before the end of a six-week period of monitoring (Figure 3). The range of detected luminescence was from 0 to  $4.88\times 10^9$  photons (average of  $9.56\times 10^8$  and standard deviation of  $1.56\times 10^9$ ). Figure 4 shows imaging by both BLI (Figure 4A) and radiography (Figure 4B) for a representative mouse monitored weekly. At days 18 and 31, no bone remodeling was observed although tumor growth was detected by BLI. By day 38, intratibial tumors had

begun to induce bone remodeling within the cortical bone that was visible by radiography. These lesions continued to develop into mixed osteolytic/osteoblastic lesions by day 52 and showed very strong luminescence.

We investigated whether the radiographic changes, histology of primary and metastatic lesions and the response to drug treatment of this mouse xenograft model showed similarities to those of OSA in human patients. As determined by radiography, osseous lesions produced by OS187-luc OSA cells formed mixed osteolytic/osteoblastic tumors (Figure 4). Histological findings of all seven tumors were consistent with undifferentiated primary bone high-grade sarcomas (Figure 5A). The cells were plump and spindle-shaped with vesicular chromatin and prominent nucleoli, and had a very high mitotic rate. Zones of necrosis were present. Figure 5B shows a human primary bone sarcoma showing similar brisk mitotic activity and spindle-shaped cells. On examination at necropsy, primary tumors were large and well-vascularized with substantial tributaries from major vessels going to the tumors. In some cases, significant necrosis was present. Tumors had progressed in the tibial metaphysis and also had considerable soft tissue growth (data not shown).

To evaluate the ability of this model to develop metastases, twelve male nude mice were orthotopically injected with exponentially growing OS187-luc cells. Of these, six mice developed pulmonary metastases an average of six weeks following injection. One mouse died suddenly of unknown causes and was not necropsied. BLI was carried out on all remaining mice and pulmonary metastasis was confirmed by necropsy and/or histology. Figures 5E and F show BLI of mice orthotopically injected with OS187-luc. Figure 5E shows a mouse with bioluminescence in the primary tumor with no detectable bioluminescence in the lungs that also showed no macroscopic or histological evidence of pulmonary metastasis at necropsy (data not shown). Figure 5F shows a mouse with bioluminescence in the primary tumor and also the lungs bilaterally. Macrometastases were visible at necropsy in all mice that showed *in vivo* bioluminescence in the region of the lungs. Figure 5G shows normal mouse lung and Figure 5H shows a lung from a mouse with pulmonary metastasis. These metastases were ovoid in shape and growing in the lung parenchyma. In some cases, the metastases comprised as much as a third of the lung. Histologically, lung tumors (Figure 5C) showed identical features to the primary tumor in the tibia (Figure 5A). Figure 5D shows a human OSA pulmonary metastasis with similar spindle-shaped cells and high mitotic activity and normal pulmonary parenchyma on the right for comparison.

In order to determine whether this system would be useful for testing new therapeutic agents, we first wanted to determine whether a response to a drug that is known to

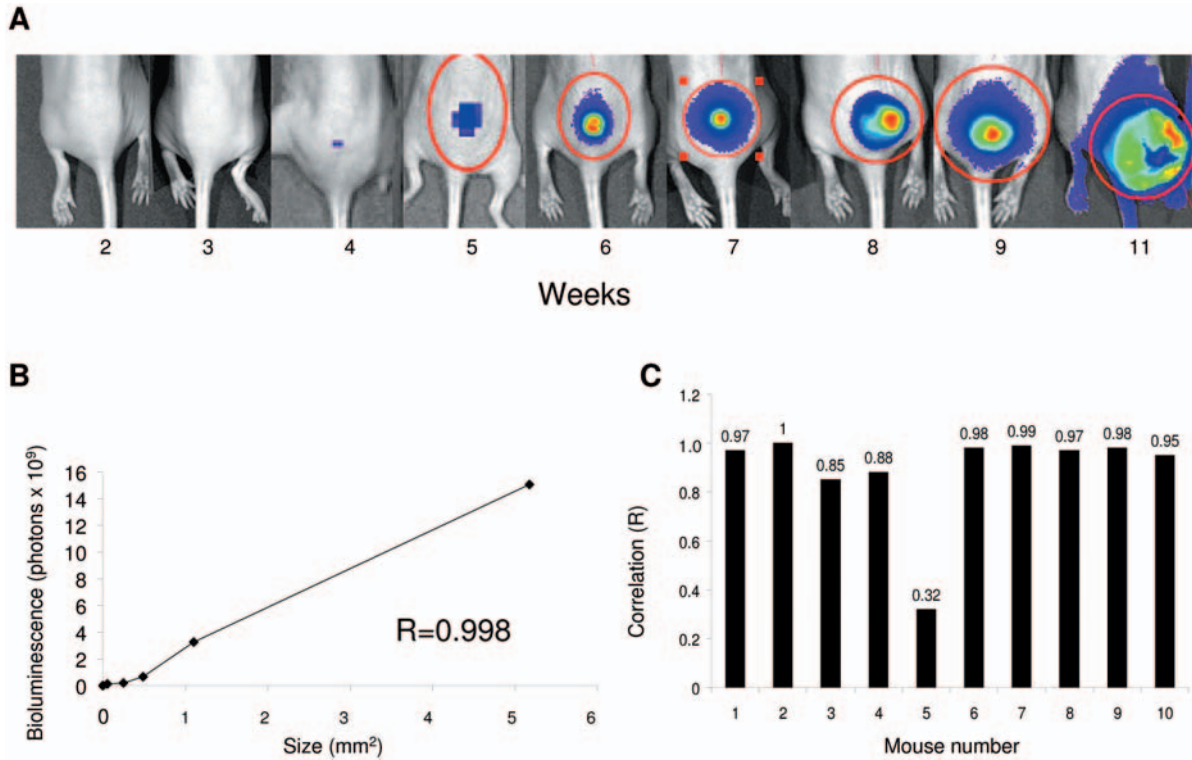


Figure 1. Bioluminescent imaging of subcutaneous growth of OS187-luc correlates with caliper measurement. A, Bioluminescent images taken weekly of a representative mouse. The colors correlate with bioluminescent intensity ranging from red (highest intensity), yellow, green, blue to purple (lowest intensity). B, Correlation between subcutaneous tumor volume measured by calipers and bioluminescent imaging in a representative mouse. C, Correlation between subcutaneous tumor growth measured by calipers and bioluminescent imaging in ten mice.

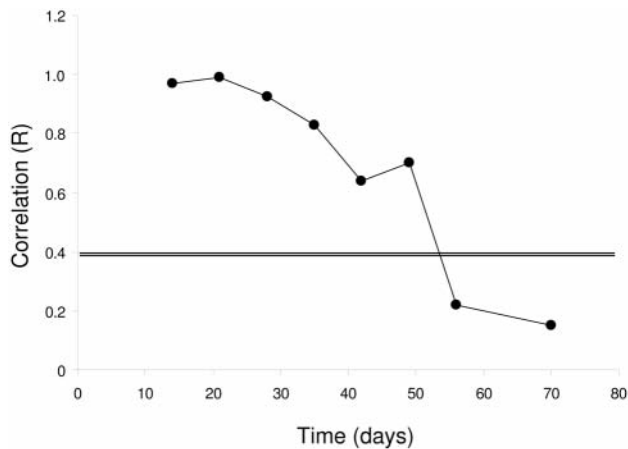


Figure 2. Correlation of tumor volume measured by calipers and BLI in ten mice over time. The data for all mice alive at each time point were used to determine the Spearman's rank correlation between tumor volumes estimated using BLI and calipers for each time point.

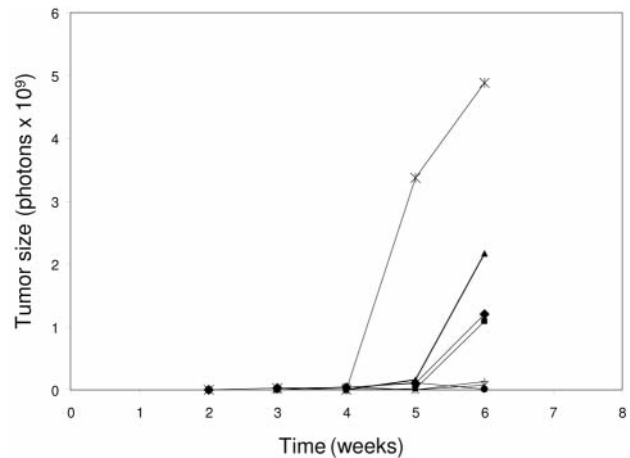


Figure 3. Tumor growth in ten mice monitored by BLI following orthotopic injection of OS187-luc.

effect OSA tumor growth in humans could be detected. Cisplatin has been used to treat OSA in humans for approximately 30 years albeit with serious side-effects. Cisplatin has not previously been used in a mouse model

of human OSA, but has been used in nude mouse xenograft models of human gastrointestinal tract tumors and breast cancer (10) (James Rae, personal communication). The maximum tolerated dose in nude

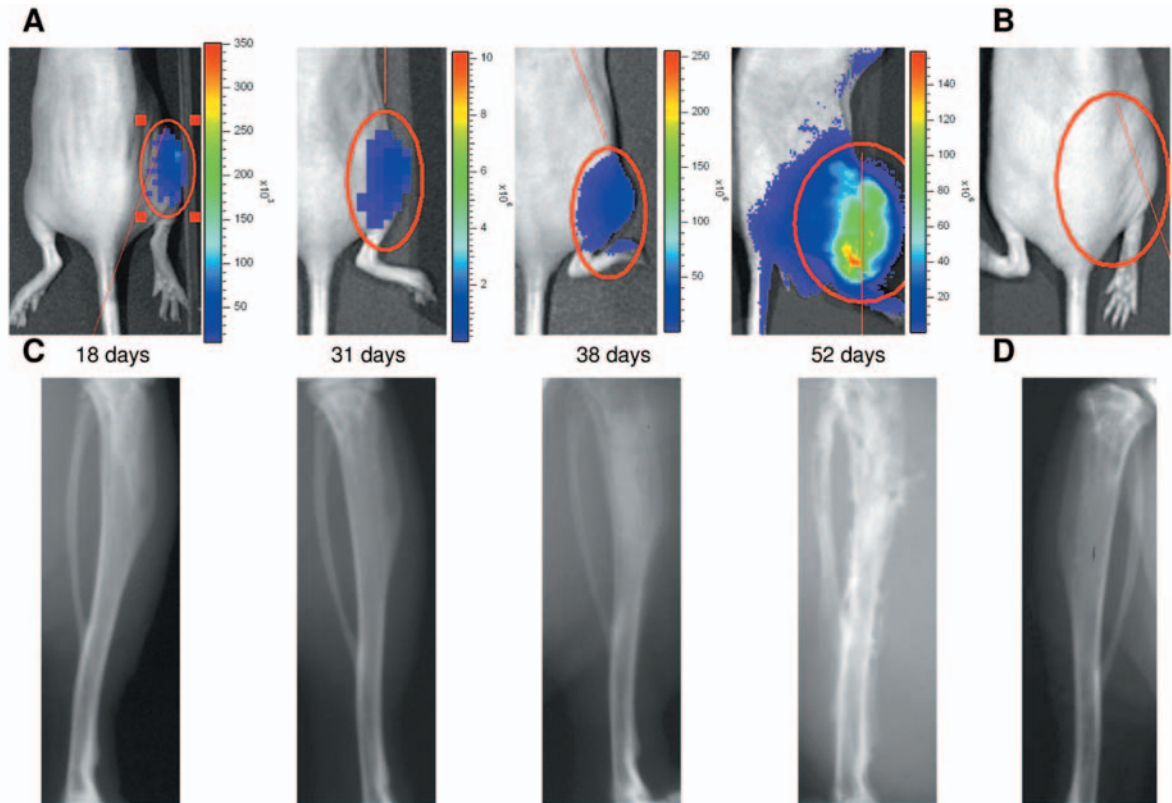


Figure 4. Tumor growth by BLI following orthotopic injection of OS187-luc. A, Tumor growth in a representative mouse in detected by BLI at 18, 31, 38 and 52 days. B, BLI of a mouse that did not show tumor growth by 52 days. C, Tumor growth followed by radiography in the same representative mouse at 18, 31, 38 and 52 days. D, Radiograph of the uninjected leg of the same mouse at 52 days.

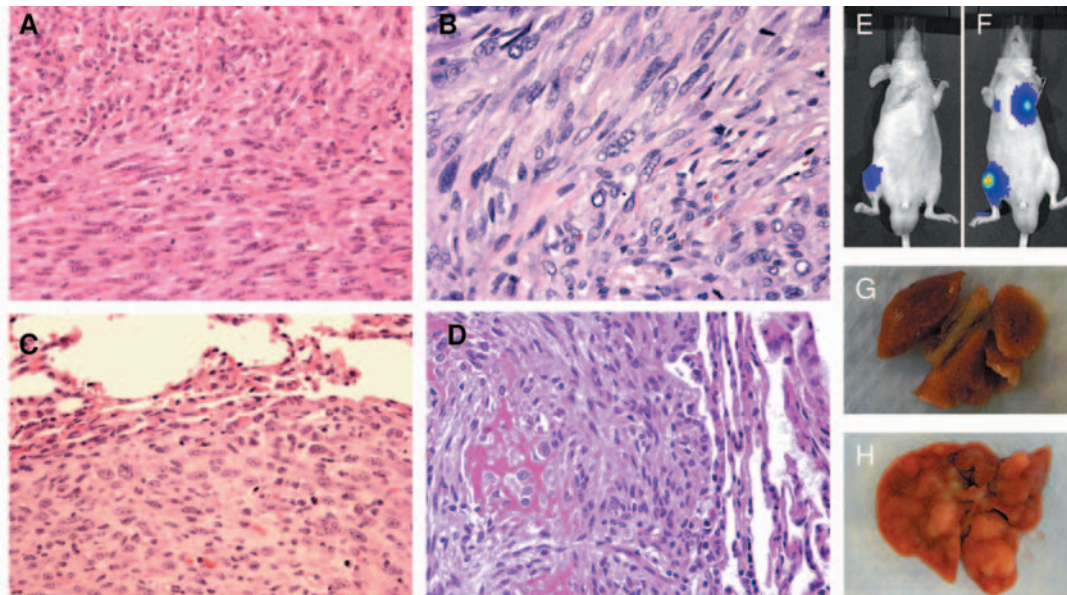


Figure 5. Detection of primary tumor and pulmonary metastasis following orthotopic injection of OS187-luc. A-B, Primary tumor of a representative mouse ( $\times 200$ ) and a human patient ( $\times 400$ ), respectively, stained with hematoxylin/eosin. C-D, Pulmonary metastases of a representative mouse ( $\times 200$ ) and a human patient ( $\times 200$ ), respectively, stained with hematoxylin/eosin. E-F, Bioluminescent imaging of two representative mice. E, Primary tumor growth with no detectable bioluminescence in the lung area. F, Bilateral bioluminescence in the lung area that was confirmed as pulmonary metastasis. G-H, Gross appearance of the lung of representative mice: G, normal mouse lung; H, lung showing extensive pulmonary metastasis.

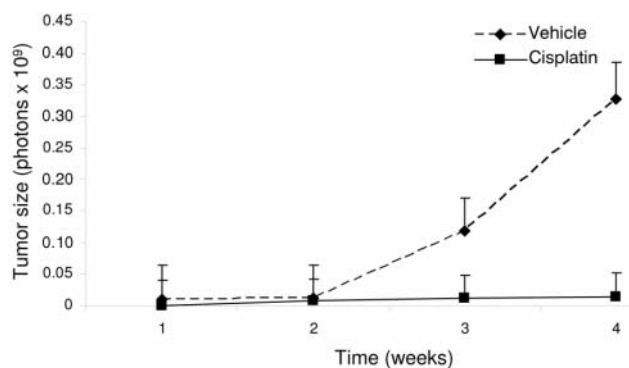


Figure 6. The effect of cisplatin treatment on tumor growth following orthotopic injection of OS187-luc. Cisplatin-treated,  $n=6$ ; vehicle-treated,  $n=9$ , ( $p>0.05$  at weeks 1, 2, and 3 and  $p<0.0001$  at week 4).

mice determined by these previous studies was 8.0 mg/kg administered once weekly intraperitoneally.

Mice were orthotopically injected in the right tibia with OS187-luc cells. The 22 mice were divided into two groups: Group A (12 mice) and Group B (10 mice). One week after OSA cell injection and before treatment, six mice in Group A and five mice in Group B had developed tumors as determined by BLI. At this point, all Group A mice were treated with 8.0 mg/kg cisplatin and all Group B mice were treated with vehicle alone administered intraperitoneally once weekly. The classic toxic side-effects of cisplatin therapy are renal, gastrointestinal and neurological. Mice were monitored for behavioral or postural signs of neurotoxicity and weight loss resulting from decreased appetite. Mice were to be euthanized if more than 25% of the original body weight was lost, there were gross signs of nephrotoxicity, or tumors began to ulcerate, however no mice showed any of these symptoms. At the end of the four-week study period, one vehicle-treated mouse and six cisplatin-treated mice were excluded from the analysis because they had failed to grow tumors. It is possible, given the differences in the numbers of mice failing to grow tumors between the control and treatment groups, that the cisplatin treatment prevented some of the mice from developing measurable tumors and therefore the effect of the cisplatin treatment may have been underestimated. Mice were monitored weekly using BLI to assess growth of the primary tumor in the presence or absence of cisplatin treatment. None of the mice in this experiment showed pulmonary metastasis. Cisplatin reduced tumor growth compared to vehicle treatment as detected by BLI (Figure 6). The control group tumors at 4 weeks (mean= $3.28 \times 10^8$ ) were significantly larger than the cisplatin group (model estimate= $1.39 \times 10^7$ ) ( $p$ -value $<0.0001$ ).

## Discussion

In the current study, a model of OSA was developed that used human cells implanted orthotopically, developed spontaneous pulmonary metastases from the primary tumor and demonstrated a response to a chemotherapeutic agent as determined by BLI. While several mouse models of human OSA have been reported previously, the one described here is unique in that orthotopic injection of non-oncogene transformed human cells that express luciferase and show pulmonary metastasis was developed and used (11-15). The expression of luciferase allows the use of non-invasive BLI, which we demonstrate to be a powerful tool for following OSA tumor progression and pulmonary metastasis. This model permits monitoring of tumor sites in the same cohort of animals over time. Primary tumor growth in mouse models of OSA has customarily been measured using calipers; however, there are some disadvantages to this method. One of these is the change in tumor shape during growth which can make measurements imprecise, especially when more than one technician performs the measurements. BLI has the advantage that measurements can be taken at serial time points from the same individual animal allowing a real-time assessment of the effectiveness of potential therapeutic agents (16). Strong correlation has been reported in some model systems of other types of cancer between photon emission and tumor burden (17-19). However, others have reported that attenuation of light emission with increased tissue depth and necrosis and changes over time in luciferin substrate circulation in individual mice following intraperitoneal injection can cause difficulties in obtaining a significant correlation between tumor burden and luminescence (20). In order to determine whether measuring tumor volume as a function of bioluminescence was at least as accurate as the traditional measurement by calipers, we directly compared both methods using the same group of mice. Our results suggest that there is good correlation between BLI and caliper measurement for measurement of primary tumor volume in most mice. However, the correlation decreases as more time elapses from the tumor cell injection and the tumor becomes larger in volume. It is possible that tumor necrosis may account for loss of correlation at later time points. We found regions of necrosis in most larger tumors upon necropsy. Notably, tumor volume measured by calipers will include non-viable necrotic tumor within the tumor mass, whereas BLI will measure only viable tumor. Thus, BLI may actually have an advantage over caliper measurement in these cases as only viable tumor cells are measured. Moreover, we demonstrate in this model that BLI allows detection of the tumor at least a week and a half before a palpable tumor can be felt and measured by calipers. This will allow a more rapid assessment of tumor growth and potential response to new therapeutic agents. Significantly, our results show that BLI can be used to detect OSA lung metastases in mice without surgical methods.

This allows a real-time assessment of the extent of metastasis.

This model exhibits OSA growth in humans without our having significantly altered the cells by genetic manipulation. Specifically, the model shows similarities in radiography, histology of primary tumors and metastases, and the response to drug treatment. As shown by clinical radiography, OSA lesions can appear purely osteolytic (approximately 30% of cases), purely osteoblastic (approximately 45% of cases), or a mixture of both. The osseous lesions produced by OS187-luc OSA cells formed mixed osteolytic/osteoblastic tumors and therefore accurately reflect the clinical progression in bone of this disease.

The morphological appearance of OSA is not homogeneous and can vary from classic OSA that produces osteoid and comprises 45% of cases, to chondroblastic (27%), anaplastic (17%), and fibroblastic (9%) that produce very little osteoid, telangiectatic that produces minimal to undetectable osteoid, and other osteosarcomas (2%) (21). The mouse primary tumors and pulmonary metastases described here can be classified as osteosarcomas that are at this stage phenotypically undifferentiated sarcomas that do not produce osteoid.

Response to cisplatin treatment was seen in this mouse model. Although the dose was higher in the mice (8 mg/kg) than is usually administered to human patients (3 mg/kg), the drug was very well tolerated and none of the mice showed signs of serious side-effects. Differences in drug dosage between mice and humans are not unusual. This verifies that response to a drug known to cause tumor regression in humans elicits a similar response in mice and suggests that this model will be useful in testing the effectiveness of new drugs.

Additional and improved animal models of OSA including the one described here will facilitate the discovery of pathways involved with OSA progression and metastasis. These models will also allow the testing of better targeted drugs and small molecule inhibitors as therapies for OSA, which may avoid the serious side-effects that plague older drugs. The advances made through the use of these models could greatly improve the outcome for patients with OSA. Because of its rapid disease progression in terms of primary tumor growth and metastasis coupled with a propensity to form tumors orthotopically and metastasize to the lungs and the ability to use non-invasive imaging, this model will aid in the development of new diagnostic and prognostic markers and new therapeutic strategies for OSA, a currently intractable disease.

## Acknowledgements

This work was supported by the Robert & Heather Ulrich Research & Patient Care Fund and National Cancer Institute Grants P01 CA093900. The authors thank David Lucas for reviewing the histology of the tumors and Scott Schuetze, Laurence Baker and James Rae for helpful discussions.

## References

- 1 Marina N, Gebhardt M, Teot L and Gorlick R: Biology and therapeutic advances for pediatric osteosarcoma. *Oncologist* 9(4): 422-441, 2004.
- 2 Herzog CE: Overview of sarcomas in the adolescent and young adult population. *J Pediatr Hematol Oncol* 27(4): 215-218, 2005.
- 3 Ferguson WS, and Goorin AM: Current treatment of osteosarcoma. *Cancer Invest* 19: 292-315, 2001.
- 4 Bacci G, Bertoni F, Longhi A, Ferrari S, Forni C, Biagini R, Bacchini P, Donati D, Manfrini M, Bernini G and Lari S: Neoadjuvant chemotherapy for high-grade central osteosarcoma of the extremity. Histologic response to preoperative chemotherapy correlates with histologic subtype of the tumor. *Cancer* 97(12): 3068-3075, 2003.
- 5 Sluga M, Windhager R, Lang S, Heinzl H, Bielack S and Kotz R: Local and systemic control after ablative and limb sparing surgery in patients with osteosarcoma. *Clin Orthop Relat Res* 358: 120-127, 1999.
- 6 Tsuchiya H, Kanazawa Y, Abdel-Wanis ME, Asada N, Abe S, Isu K, Sugita T and Tomita K: Effect of timing of pulmonary metastases identification on prognosis of patients with osteosarcoma: the Japanese Musculoskeletal Oncology Group study. *J Clin Oncol* 20(16): 3470-3477, 2002.
- 7 Whiteford CC, Bilke S, Greer BT, Chen Q, Braunschweig TA, Cenacchi N, Wei JS, Smith MA, Houghton P, Morton C, Reynolds CP, Lock R, Gorlick R, Khanna C, Thiele CJ, Takikita M, Catchpoole D, Hewitt SM and Khan J: Credentialing preclinical pediatric xenograft models using gene expression and tissue microarray analysis. *Cancer Res* 67(1): 32-40, 2007.
- 8 Hall CL, Dai J, van Golen KL, Keller ET and Long MW: Type I collagen receptor (alpha 2 beta 1) signaling promotes the growth of human prostate cancer cells within the bone. *Cancer Res* 66(17): 8648-8654, 2006.
- 9 Davol P and Frackelton AJ: Targeting human prostatic carcinoma through basic fibroblast growth factors in an animal model: characterizing and circumventing mechanisms of tumor resistance. *Prostate* 40: 178-191, 1999.
- 10 Imaizumi M, Kondo T, Taguchi T, Hattori T, Abe O, Kitano M and Wakui A: A standardized method of using nude mice for the *in vivo* screening of antitumor drugs for human tumors. *Surg Today* 23(5): 412-419, 1993.
- 11 Berlin O, Samid D, Donthineni-Rao R, Akesson W, Amiel D and Woods VL Jr: Development of a novel spontaneous metastasis model of human osteosarcoma transplanted orthotopically into bone of athymic mice. *Cancer Res* 53(20): 4890-4895, 1993.
- 12 Jia SF, Worth LL and Kleinerman ES: A nude mouse model of human osteosarcoma lung metastases for evaluating new therapeutic strategies. *Clin Exp Metastasis* 17(6): 501-506, 1999.
- 13 Dass CR, Ek ET, Contreras KG and Choong PF: A novel orthotopic murine model provides insights into cellular and molecular characteristics contributing to human osteosarcoma. *Clin Exp Metastasis* 23(7-8): 367-380, 2006.
- 14 Dass CR, Ek ET and Choong PF: Human xenograft osteosarcoma models with spontaneous metastasis in mice: clinical relevance and applicability for drug testing. *J Cancer Res Clin Oncol* 133(3): 193-198, 2007.

- 15 Luu HH, Kang Q, Park JK, Si W, Luo Q, Jiang W, Yin H, Montag AG, Simon MA, Peabody TD, Haydon RC, Rinker-Schaeffer CW and He TC: An orthotopic model of human osteosarcoma growth and spontaneous pulmonary metastasis. *Clin Exp Metastasis* 22(4): 319-329, 2005.
- 16 El-Deiry WS, Sigman CC and Kelloff GJ: Imaging and oncologic drug development. *J Clin Oncol* 24(20): 3261-3273, 2006.
- 17 Douma S, Van Laar T, Zevenhoven J, Meuwissen R, Van Garderen E and Peeper DS: Suppression of anoikis and induction of metastasis by the neurotrophic receptor TrkB. *Nature* 430(7003): 1034-1039, 2004.
- 18 Jenkins DE, Oei Y, Hornig YS, Yu SF, Dusich J, Purchio T and Contag PR: Bioluminescent imaging (BLI) to improve and refine traditional murine models of tumor growth and metastasis. *Clin Exp Metastasis* 20(8): 733-744, 2003.
- 19 Jenkins DE, Yu SF, Hornig YS, Purchio T and Contag PR: *In vivo* monitoring of tumor relapse and metastasis using bioluminescent PC-3M-luc-C6 cells in murine models of human prostate cancer. *Clin Exp Metastasis* 20(8): 745-756, 2003.
- 20 Lyons SK: Advances in imaging mouse tumour models *in vivo*. *J Pathol* 205(2): 194-205, 2005.
- 21 Abeloff M, Armitage J, Lichter AS and Niederhuber JE (eds.). *Clinical Oncology*, 2nd ed. New York Churchill Livingstone/Harcourt Brace & Company: 2000.

*Received March 23, 2009*

*Revised June 10, 2009*

*Accepted June 12, 2009*